Economic Sciences
https://economic-sciences.com
ES (2025) 21(1), 153-173 | ISSN:1505-4683

Cascade Hybrid-Deep Learning Driven Multi-Factor Sensitive Landslide Prediction System

Rajesh B
Senior Lecturer, School of Management, Mahindra University, Hyderbad, Telangana, India
Rajesh.balarama@mahindrauniversity.edu.in, https://orcid.org/0000-0001-7011-5338

Abstract- *In recent years, the world has witnessed exceedingly high dynamism in nature's behavior including tsunami, landslide, flood and fire. More specifically, the events of landslide have become frequent globally, thus claiming thousands of innocents lives every year. Landslide prediction requires understanding varied factors like geological, geomorphometric, soil, environmental and precipitation features for the specific geography, eventually becomes a complex task. The increasing severity of landslide has alarmed academia-industry to develop robust and reliable landslide susceptibility mapping and allied prediction solution. Though, advanced software computing, satellite technology and data analytics has broadened the horizon for landslide prediction; however, it requires optimality of features as well as the learning environment. In the past, numerous approaches are developed by using precipitation features like rainfall for landslide prediction; however, merely applying standalone feature can't ensure reliability of the system, especially when global climate pattern is undergoing decisive change due to global warming. Considering these factors, this paper proposes a robust hybrid-deep learning driven multi-factor sensitive landslide prediction system. The proposed model applies multiple landslides influencing factors like geological, geomorphometric, soil, environmental and precipitation to train a strategically designed hybrid deep learning model for landslide prediction. To ensure computational efficacy, the landslide inventory factors were processed for significant predictor test, which helped retaining the optimal set of influencing factors collected from the GIS benchmarks. To train the selected features optimally for learning and prediction, a cascade architecture was used, with Long Short-Term Memory (LSTM) networks retrieving local features and Bidirectional-LSTM (Bi-LSTM) networks retaining long-term dependency features. The suggested model achieves landslide prediction accuracy of 96.38%, precision of 95.19%, recall of 95.33%, and F-Measure of 95.56%, according to the simulation data. The suggested model is robust towards real-time applications, as confirmed by the mean average error of 0.1109 and the root mean square error value of 0.1860.*

Keywords— *Landslide Prediction, Influencing Factor, Hybrid Deep Learning, BI-LSTM, Susceptibility Mapping.*

I. INTRODUCTION

In recent years, the world has witnessed exceedingly high dynamism in nature's behavior including tsunami, landslide, flood and fire. More specifically, the events of landslide have become frequent globally, thus claiming thousands of innocents lives every year. Landslide prediction requires understanding varied factors like geological, geomorphometric, soil, environmental and precipitation features for the specific geography, eventually becomes a complex task. The increasing severity of landslide has alarmed academia-industry to develop a reliable landslide susceptibility mapping and allied prediction solution. In the last few years, landslide susceptibility mapping and prediction has emerged as a vital tool for identification of landslide regions and its impact. It has been helping both environmental monitoring agencies as well as government to make proactive plans and land-use decisions. In fact, guaranteeing optimality of landslide risk prediction model is a challenging task, especially when nature's behavior remains non-linear due to global warming conditions. However, identifying and modelling the landslide influencing factors for a specific geography can help designing a landslide prediction model with robust data analytics. Yet, retaining the optimal set of landslides influencing factors remains a challenge for academia-industries due to costly satellite imagery services, continuous temporal data demands and spatial geo-stationary as well as dynamic information demands [1][2]. In addition to the landslide inventory preparation, the ambiguity over temporal and geographical details makes any prediction model confines to retain reliability aspects. The stereotyped quantitative assessment of the landslide influencing factors on the actual sites is infeasible due to exhaustive

measurement. Under such manual measurements, the likelihood of human errors cannot be avoided. Moreover, nature being dynamic and abstracted in nature can't be predicted merely on the basis of certain superficial parameters measured through human manual measurements. In this case, identifying sufficiently large influencing factors which could have direct or indirect impact on landslide susceptibility is inevitable towards landslide risk prediction. In the last few years, the rise in sensor technologies, satellite imagery services and other internet of things (IoT) tools have played decisive role in collecting different environmental parameters like geological, geomorphometric, soil, environmental and precipitation and other derived variables, which can be applied for automated analysis for landslide susceptibility mapping and risk prediction.

Typically, the landslide susceptibility or risk prediction encompasses landslide catalogue (consists of the different influencing factors), landslide vulnerability mapping, environmental spatio-temporal feature extraction, learning models, and model evaluation [3][4].

Precise measurements taken by high-tech GPS and GIS systems often include the landslide's area, position, locations, and parametric boundaries, all of which are included in the landslide catalogue [5][6]. Remote sensing imagery services, such as Landsat8 TM images, digital elevation models (DEMs), aerial photography, and light detection and ranging (LiDAR), can also be used to collect environmental information associated with landslides. In addition, it is possible to think about using GIS spatial analysis, which can give hydrological assessment, map algebra, and terrain analysis [7]. In conclusion, GIS is the foundation for landslide prediction models because of its compatibility with mapping, geographic big data analysis, and related data management activities [7]. Various prediction tasks have seen a rise in the usage of GIS data in recent years [8]. The information value model [9], logistic regression [10][11], entropy index [12], certainty factor [13][14], analytic hierarchy process [15][16], and a few others are based on GIS data that can be used to predict landslides. It is worth noting that even these state-of-the-art approaches have their limits. For example, before learning and classification, large feature data needs to be processed for a specified statistical distribution.

Additionally, the need of annotations makes them a complex approach and guaranteeing different prior knowledge demands, becomes challenging in real-time applications. Though, machine learning methods have performed better results by learning over different environmental parameters and allied (landslide) influencing factors. Their ability to learn over more complex relationship amongst the parameters as well as input-outputs make them resulting higher accuracy [17-20]. Multiple adaptive regression splines (MARS) [21][22], fuzzy logic [23][24], artificial neural networks [25], decision trees [27-29], random forests [30-32], support vector machines [33-35], rule-based approaches [36], multi-criteria evaluation techniques [37], and so on are some of the machines learning-driven solutions that have recently emerged.

However, these approaches are often criticized for their limitations such as the need of huge prior information including long-term temporal data with annotations. Additionally, these approaches can't be able to handle abstracted information learning and inter-element association to make more reliable prediction. These machine learning methods are unable to extract the underlying landslide features which can have straight or indirect impact on displacement. The recent literatures [38] also indicate that the at hand machine learning methods don't consider correlation amongst the sub-regions that makes confines reliability of the system under dynamic conditions. Moreover, the inherent issues of exhaustive computation, local minima, sensitivity to the missing data etc. confine their robustness towards landslide risk prediction. Unlike machine learning methods, deep learning approaches are found superior, especially in terms of more fine-grained feature learning, minimum convergence issues, higher accuracy and lower sensitivity towards missing data [38]. Additionally, deep learning methods are more capable of extracting inherent and deep features, which can make it potential towards landslide prediction. Moreover, the least reliance on the supplementary knowledge along with its potential to learn amongst the extracted local features for better inference makes deep learning methods suitable for at hand landslide prediction task [39-42]. Though, in the past a few deep learning methods like convolutional neural network (CNN), long and short-term memory (LSTM) and

Economic Sciences
https://economic-sciences.com
ES (2025) 21(1), 153-173 | ISSN:1505-4683

other recurrent deep models have been used for landslide prediction; however, most of the at hand solutions either use limited number of environment parameters (ex. Rainfall patterns, slope, displacement etc.) or employ mainly the local features (Ex. CNN) for learning and classification. A few approaches; though extract features using deep models, while training and classification is done over machine learning methods, which makes their efficacy suspicious, especially under real-time prediction over dynamic conditions. Consequently, a strong deep environment that can use both short-term and long-term dependence traits to forecast landslides is essential, as are additional spatio-temporal features that define the parameters that influence landslides.A landslide prediction system that is both sensitive to multiple factors and driven by deep learning is created in this research. The suggested methodology trains a strategically built hybrid deep learning model for landslide prediction by using numerous influencing factors, such as geological, geomorphometric, soil, environmental, and precipitation, as the name suggests.

To ensure computational efficacy, the landslide inventory factors were processed for significant predictor test, which helped retaining the optimal set of influencing factors collected from the GIS benchmarks. The selected features were trained over LSTM and Bidirectional-LSTM (Bi-LSTM) networks in a cascade architecture, where LSTM retrieved local features, while the later (i.e., Bi-LSTM) retained long-term dependency features to ensure optimality of feature for learning and prediction. The suggested model obtains an F-Measure of 95.45%, a recall of 96.57%, a precision of 94.37%, and an accuracy of 96.72% when it comes to landslide prediction. Furthermore, the suggested model is robust towards real-time applications, as confirmed by the mean average error of 0.0862 and root mean square error values of 0.1358.Here is a breakdown of the remaining sections of the manuscript that has been provided. After introducing the relevant literature in Section II, the following section defines the problem. The data preparation and deep learning driven prediction model are presented in Section IV. Section V then follows with results and analysis. Section VI delves into the discussion of the overall research conclusions and inferences. The list of sources consulted throughout this work is detailed in the citation section.

II. Related Work

This section discusses the key recent approaches developed towards landslide susceptibility mapping and risk prediction. The key purpose of landslide risk prediction and allied susceptibility mapping is to identify the suitable assessment metrics which can have the decisive impact on landslide probability and deploy them to model an automated solution for risk prediction. Data being the crucial component behind landslide risk prediction models have attracted academia-industries to achieve suitable set of influencing factors for further (risk) analysis. In reference to the hypothesis stating that the use of IoT technologies can enable multi-sensory driven (influencing) landslide data (say, influencing factors) collection, Joshi et al. [1] applied edge computing technique to collect landslide data for risk analysis. Li et al. [2] on the other hand performed quantitative assessment to identify landslide influencing factors. To be more precise, the authors used GIS [2] technology to determine the rainfall intensity-duration threshold condition, and then applied it to the landslide probability model. Nevertheless, according to data collected from landslide events by NASA and other environmental monitoring agencies, such as the Geographical Survey of India (GSI), a wide range of factors, such as slope pattern, soil type, curvatures, solar radiation, valley depth (VD), terrain ruggedness index (TRI), vector ruggedness measure (VRM), stream power index (SPI), topographic wetness index (TWI), length slope (LS), topographic position index (TPI), land use, normalized difference vegetation index (NDVI), lithology, soil, distance to fault, distance to river, distance to road, fault density, river density, road density, etc. [43]. Remondo et al. [44] used spatial data to estimate the likelihood of landslides; they developed quantitative hazard models by plugging in historical landslide information, landslide frequency, and size. Landslide risk prediction using stacked auto-encoder (SAE) was done efficiently by Tan et al. [4]. The authors asserted that their method outperformed traditional machine learning techniques such as radial basis functions (RBF) and artificial neural networks (ANN) [45].

Goyes-Peñafie [46] applied landslide susceptibility index by employing both discrete as well as continuous data for landslide susceptibility prediction. The authors applied logistic regression (LR) and weights of evidence (WoE) approach to perform feature learning and classification. Though, to improve prediction reliability, especially under missing data conditions, Utomo et al. [46] applied LSTM deep network for landslide prediction. Despite their efforts, the accuracy of 90% questions its reliability for real-time applications. Though, the efforts by Liu et al. [48] resulted better performance by applying LSTM with gated recurrent units for landslide displacement analysis. Srivastava et al. [49] applied rainfall information (i.e., rainfall threshold index) for landslide prediction. To predict rainfall and, by extension, the likelihood of landslides, their method involved mapping the acquired rainfall index or measurements to several machine learning algorithms, such as back-propagation neural networks (BPNN), support vector regression (SVR), and long short-term memory (LSTM).

The IoT sensory driven rainfall-induced landslide prediction model was developed by Khaing and Thein [50], where the collected rainfall measurements and corresponding thresholds were applied to LSTM network for landslide prediction. Napoli et al. [51] considered a set of 13 predisposing influencing factors, which were later trained by using ANN, generalized boosting model and the maximum entropy approach to perform landslide susceptibility mapping and allied risk prediction. To improve prediction reliability, Dou et al. [52] designed an ensemble learning approach encompassing SVM with Boosting and staked learning framework for landslide risk prediction. Liang et al. [53] assessed different landslide susceptibility mapping approaches, where they found that the use of gradient boosting decision tree (GBDT) algorithm can yield superior results; yet the authors failed in exploiting large set of landslides influencing factors. Additionally, it doesn't consider long-term dependency amongst the influencing factors to make learning and prediction more realizable. Ma et al. [54] assessed relative performance of the image-based landslide risk prediction model, landslide sensitivity analysis and landslide early warning systems by applying machine learning methods. Despite being a review effort, the authors failed in identifying suitable set of influencing factors towards landslide prediction. Liao et al. [55] applied grey wolf optimization method processed over trend displacement and periodic displacement information to perform landslide risk analysis. The authors found that the periodic displacement can be an indicator for landslide risk models. In contrast, Li et al. [56] used an autoregressive motion-averaged time series model to estimate parameters linked to landslides through auto-correlation. In addition, the inferred displacements were also fitted using the parametric correlation approach. After that, in order to anticipate the risk, we looked at the correlation between the influencing factor and the values of landslide displacement. The important non-stationary features associated with landslide displacement are ignored by classical landslide prediction models, according to Huang et al. [57].

They applied a discrete wavelet transform (DWT) feature driven extreme learning machine (ELM) which was designed on the basis of the chaos theory to predict landslide displacement. The authors applied time-series data pertaining to the displacements in landslide for risk prediction. However, it failed in exploiting other geological conditions and precipitations which cause displacement. Considering such limitations, Research by Cao et al. [58] made use of correlations in response between data on landslide deformation, rainfall, reservoir water level, and groundwater level.

The landslide influencing factors were trained over ELM to perform risk prediction. Moreover, an empirical mode decomposition driven ELM model was designed by Cheng Lian et al. [59] to perform landslide displacement prediction. The other neuro-computing variant named BPNN was applied in [60] to learn slope information to predict landslide slope deformation analysis. Despite higher accuracy, training a model with merely one slope pattern data can't provide a reliable risk analysis solution. Moreover, the aforesaid machine learning driven solutions require a large set of input data and corresponding annotations to perform landslide prediction, which can be very complex and challenging task in real-time applications. The ability of deep networks for fine-grained data learning over limited inputs with minimally possible hyper-parameters tuning make them suitable for at hand LSM and allied risk prediction tasks.

Considering the limitations of the existing machine learning-based methods, recently a few efforts have been made by exploiting deep network [61-66]. Zhang et al. [61] designed an attention based temporal CNN for landslide risk prediction. To improve reliability, the authors focused on exploiting landslide instability margins (LIMs) for which an attention-based CNN was designed. Here, attention model was applied to retain long-term dependency. Pairwise separable deep features were trained by using random forest classifier (Yilmaz et al. [62]). Xu et al. [63] developed a model for landslide displacement prediction using variational mode decomposition (VMD) and long short-term memory (LSTM). To begin, this approach used VMD to break down the total displacement data, which then yielded time-series environmental effect variables like rainfall and water level. In order to conduct risk prediction, these details were then trained over LSTM. The use of deep learning and machine learning techniques to learn about geo-environmental variables like lithology, soil texture, land use/cover, slope angle, slope aspect, topographic wetness index, distance from road, distance from streams, distance from lineaments, convergence index, profile and plan curvatures, and more was recently demonstrated in a case study of landslide risk assessment in the Indian western ghats [64]. In spite of a lot of work, the authors were unable to keep long-term dependency, which would have made the system more reliable in the long run. For the purpose of landslide prediction in Pakistan, Mubashar et al. [65] utilized a number of characteristics, such as surface pressure, specific humidity, surface runoff, rainfall, root level soil moisture, 10 cm soil moisture, average temperature, transpiration, wind speed, aspect, slope, and elevation. In order to forecast landslides, the authors used LSTM to extract features, and then they used ANN-based classification. After using artificial neural networks (ANNs) for classification, Liu et al. [66] used gated recurrent units (GRUs) to learn spatial features.

Though, GRU acted as a textural feature extraction model for further learning; however, the limited features can confine overall performance.

III. Problem Formulation

Landslide prediction has emerged as one of the most decisive and significant approaches for environmental geostatistical monitoring and surveillance. The rising events of landslide globally and resulting loss-of lives and economy has alarmed researchers to achieve a robust landslide prediction system. In this reference, though a number of efforts have been made in the past; however, the solutions based on machine learning and deep networks have performed satisfactorily. Despite innovations, machine learning methods often undergo adversaries like the need of huge annotations, local minima and convergence that confine them for a real-time solution, especially with large datasets encompassing geological, geomorphometric, soil, environmental and precipitation. Though, to alleviate it, in the past a few machines learning-based methods are proposed with reduced number of landslides influencing factors such as rainfall, slope, vegetation, soil types, etc. However, most of the at hand solutions either undergo limitations because of limited features (say, landslide inventory or allied influencing factors) or inability to learn optimally over large inputs. On the contrary, applying image-data has always remained costly and computationally exhaustive. To alleviate it a robust solution improving both features as well as computing environment can be vital. The methods applying multiple parameters have performed reasonably better in comparison to the machine learning based landslide susceptibility mapping approaches. However, almost major solutions learn over the local features derived from each (landslide) influencing factor, and hence their (say, inter-component or between the influencing factors) long-term dependency has never been addressed. On the contrary, under uncertain nature merely applying shallow features or superficial (local) features can't guarantee optimality of a solution. Moreover, under multi-parametric setup (say, with geological, geomorphometric, soil, environmental and precipitation features and others) retaining computational efficacy is equally important. In sync with these key research challenges and allied scopes, in this paper a hybrid-deep learning driven multi-factor sensitive landslide prediction system was developed. The proposed model focused on improving both features and computing environment. As feature environment a large number of influencing factors were obtained from the landslide inventory data. Moreover, the use of Wilcoxon Rank sum method retained optimal set of influencing factors towards landslide prediction. In particular, sixteen factors were identified by the proposed feature selection model as

Economic Sciences
https://economic-sciences.com
ES (2025) 21(1), 153-173 | ISSN:1505-4683

having an impact. These factors include orientation, slope angle, height above sea level, curvature, profile curvature, plan curvature, solar radiation, valley depth, terrain ruggedness index, stream power index, topographic wetness index, length slope, topographic position index, land use, normalized difference vegetation index, lithology, soil, and rainfall. A hybrid deep network consisting of LSTM and Bi-LSTM was fed the retrieved features as input. This research utilized Bi-LSTM, which was trained on LSTM extracted features to retain long-term dependency, as opposed to classical approaches that merely apply CNN or LSTM deep networks for feature extraction (they can merely exploit word-level local features). Consequently, the suggested LSTM and Bi-LSTM model was able to attain optimal learning and classification by being trained over both local and global features, such as the long-term dependency among the influencing elements.

IV. SYSTEM MODEL

The suggested model and its related sequential implementation are covered in detail in this section. All things considered, the procedure includes these stages:

Phase-1 Data Collection

Phase-2 Significant Predictor Test

Phase-3 Landslide Influencing Factors Identification

Phase-4 Hybrid Deep Learning based Landslide Risk Prediction.

The following sections provide a comprehensive analysis of the suggested model.

A. Data Collection

The landslide inventory map and the identification of related influencing parameters are the primary topics of this part.

a. Landslide Inventory Map

This is the matter of fact that preparing the landslide inventory map information pertaining to a specific geography is a challenging task, and therefore in this work the secondary data availble at the different standard benchmarks including Kaggle, NASA and Geographical Survey of India (GSI) were taken into consideration. In this reference, at first that landslide distribution map was prepared before performing landslide modelling, as this study hypothesizes that the future probability of landslide in future is highly in sync with the (landslide) conditions in the past [67]. Thus, learning over the previous landslide conditions the future probability of landslide can be predicted by exploiting different spatio-temporal information. It signifies that learning over specific topographic, geological, hydrogeological and climatic conditions for a target region, one can predict the likelihood of landslide. A recent study by Galli et al. [68] has inferred that the scalability and perfection of a landslide inventory map can have the decisive impact on accurate landslide risk prediction models. Though, the literatures identified a total of 118 landslide influencing factors, there used to be certain more decisive element having impact on landslide probability. This study applies the data constructs as suggested in [69], where the authors have applied 175 landslide locations; however, post significant predictor test a total of 16 features were retained. A snippet of these selected features is given as follows:

b. Landslide Influencing Factors

For the purpose of landslide risk prediction, this study considered sixteen features for additional learning and classification. These key features are:

1. *Slope angle,*
2. *Aspect,*
3. *Elevation above sea level,*
4. *Curvature,*
5. *Solar radiation,*
6. *Valley depth (VD),*
7. *Terrain ruggedness index (TRI),*
8. *Vector ruggedness measure (VRM),*
9. *Stream power index (SPI),*
10. *Topographic wetness index (TWI),*
11. *Topographic position index (TPI),*
12. *Land use,*
13. *Normalized difference vegetation index (NDVI),*
14. *Lithology,*
15. *Soil,*
16. *Rainfall.*

A snippet of these key variables is given as follows:

1. Slope Angle

A number of literatures [70][71] reveal that the likelihood of landslides is higher over steeper slope angle. In other words, with rising shear stresses the

Economic Sciences
https://economic-sciences.com
ES (2025) 21(1), 153-173 | ISSN:1505-4683

slopes turns steeper and hence increases the likelihood of landslide. The presence of soil often undergoes sliding over increasing slope angle and hence once the angle reaches more than 25 degrees, the soil starts losing grip to the ground and hence results landslide. In this work, the slope angle was obtained by means of the digital elevation model (DEM), which was classified into multiple intervals encompassing, 0–13, 14–22, 23–30, 31–42, and >43 degrees.

2. *Aspect*

Even while factors including soil moisture concentration, sunshine, dry winds, rainfall, and discontinuities are affected by the slope direction, landslides can still occur regardless of the slope direction [72]. The overall input observations were classified into multiple classes in this work. These classes included flat (1-39.00), north (39.00-79.00), northeast (79.00-119.00), east (119.00-159.00), southeast (159.00-199.00), south (199.00-239.00), southwest (239.00-279.00), west (279.00-319.00), and northwest (319.00-359.00). DEM was used to extract aspect information.

3. *Elevation*

Indirect associations are common when discussing the relationship between height and landslides; that is, landslides can be caused by elevation in conjunction with other secondary influencing parameters [73].

The altitude related influencing component of each geographic region used to be a distinct layer that gives rise to the slope instabilities. Elevation indirectly measures numerous causes giving rise to the landslides like rainfall patterns (say, annual and heavy rainfall pattern), temperature, changes in the frost conditions, ice melting, etc. [74]. Let the elevation limit of the target location be 2328 m (maximum) and 750 m (minimum), then the variance in elevation would be 1500 m. The elevation was measured using the DEM method and classified into eight groups: (1) 750-1000, (2) 1000-1200, (3) 1200-1400, (4) 1400-1600, (5) 1600-1800, (6) 1800-2000, (7) 2000-2200, and (8) 2200-2500.

4. *Curvature*

Often referred to as a curvature map, it displays the degree to which the surface deviates from a flat surface. Alterations to the convexity and concaveness of a slope can be represented using curvature maps [75]. Also, the positive concavity provides the convex-pixel surface with a representation of the slope's curvature, which in turn represents the topography's shape.

On the contrary, the negative concavity signifies the surface with the concave pixels. On the contrary, the zero concavity refers the surface with no slope and remains straight (also called Flat or Straight concavity). Thus, the aforesaid three kinds of slope shapes possess decisive impact on slope instability, especially because of surface's concentration and diffusion. Moreover, the subsurface water flow over the slopes too give rise to landslide [76]. This study used the lengths between successive topographic lines in the GIS to determine the aforementioned concavity and convexity, which are relevant to the slope's curvature map. To obtain the curvature map data mentioned earlier, we used a DEM that was specific to the area of interest. There were five groups into which the measurements fell: (1) extremely concave (51.20–3.79), (2) concave (3.79)–1.12, (3) flat (1.12)–(0.54), (4) convex (0.54)–(3.21), and (5) very convex (3.21)–(33.9).

5. *Solar Radiation*

The intensity of solar radiation is just the mean convergence per pixel over one year. Kilowatt hours per square meter is the unit of measurement. A greater amount of vapour relative to the surface of the soil is indicated by a higher value of solar radiation.

This parameter even helps in controlling the extent of vegetation on the target slope condition. With lower slope and low radiation, higher vegetation can be observed that eventually helps in stabilizing the slope. In this work ArcGIS technology with DEM method was applied to classify solar radiation pattern in the following classes: (1) 80,000–43,000, (2) 440,000–540,000, (3) 550,000–630,000, (4) 640,000–700,000, and (5) 710,000–810,000.

6. *Vector Ruggedness Measure (VRM)*

It opens the door to a method for estimating the roughness of nearby terrain. In this case, it combines data on slope and aspect into a single metric, which is then used to separate the terrain's roughness from its slope or elevation. First, 0-0.0302; second, 0.0303-0.0795; third, 0.796-0.151; fourth, 0.152-0.274; and fifth, 0.275-0.699 were the categories into which we

Economic Sciences
https://economic-sciences.com
ES (2025) 21(1), 153-173 | ISSN:1505-4683

placed the VRM map after applying DEM in SAGA GIS program.

7. Valley Depth

It is often considered one of the decisive and basic influencing factors for landslide susceptibility mapping problem. Using the SAGA GIS program, we measured the valley depth index using DEM. The following classes were obtained by exporting the values to ArcGIS: (1) 0-37.9, (2) 38-87.7, (3) 87.8-149, (4) 150-233, and (5) 234-508 m.

8. Stream Power Index (SPI)

It stands for the criteria, derived from the DEM study, that can affect the likelihood of landslides. The erosive strength of run-off from slope surfaces is also indicated. The following model is used to derive it mathematically (1).

$$SPI = A_s \times \tan\beta \quad (1)$$

In (1), A_s be the specific basin area, while the slope angle is given by $\tan\beta$. Here, we applied DEM with SAGA GIS software, and the outputs were further processed by ArcGIS to identify five different intervals in the SPI layer. These were: (1) 0–1510, (2) 1520–1600, (3) 1610–3110, (4) 3120–26,500, (5) 26,600–390,000.

9. Topographic Wetness Index (TWI)

Soil moisture distribution patterns can be described using this theoretical element, which specifies the accumulation of flow at a specific time in a watershed. Higher levels of TWI are typically used in landslide bodies, but it is generally used for topographic control of hydrological processes. According to (2), TWI was calculated mathematically.

$$TWI = Ln\left(\frac{A_s}{\tan\beta}\right) \quad (2)$$

The slope angle at a given position is denoted by tan⁡β in equation (2), and A_s is the total drainage upstream area at that point. The following categories were used to categorize TWI: (1) 0.0895-2.62, (2) 2.63-3.32, (3) 3.33-4.15, (4) 4.16-6.26, and (5) 6.26-10.70.

10. Terrain Ruggedness Index (TRI)

The triangle inequality (TRI) is defined as the height difference between a single pixel and its neighboring eight pixels, as determined mathematically in (3).

$$TRI = \sqrt{\sum_{p=1}^{8} ZMD} \quad (3)$$

For equation (3), let ZMD be the mean difference of eight pixels around each pixel and p be the number of pixels dispersed among the regions. First, 0-2.64, second, 2.65-4.75, third, 4.76-7.74, fourth, 7.75-13.4, and fifth, 13.5-44.9 were the categories into which we mapped the TRI index.

11. Topographic Position Index (TPI)

The TPI makes comparison of the height of each pixel with the specified pixel around (in the digital elevation model (DEM)). In order to calculate TPI, we used (4), which involves comparing the average height of nearby cells to the height of each individual cell in a DEM. As time goes on, the average height drops below the central value. A positive TPI indicates that the value of the region is greater than the value of the surrounding points.

On the contrary, negative TPI signifies areas lower in comparison to the corresponding surroundings. Moreover, the 0 and near-0 values signifies flat areas, with the slope nearing zero (as well as those areas with a definite slope value).

$$TPI = Z_0 - \sum_{n-1}\left(\frac{Z_n}{n}\right) \quad (4)$$

In (4), Z_0 refers the point height under assessment. The second point, Z_n, is the height of the grid, and n is the total number of nearby points that were evaluated.

In this work, TPI was classified as the following classes: (1) (-75.7)–(-9.77), (2) (-9.77)–(-2.83), (3) (-2.83)–(2.94), (4) (2.94)–(11.03), and (5) (11.03)–(71.7).

12. Land Use/Land Cover

It signifies the slope's instability that influences the land-behavior and undergoes dynamism. The GSI land use map was used to obtain the land use layer for this project. Woodland, semi-dense forest, low-dense

Economic Sciences
https://economic-sciences.com
ES (2025) 21(1), 153-173 | ISSN:1505-4683

forest, semi-dense/dense pasture, and dry-farming are the land use/cover classes categorised here.

13. Normalized Difference Vegetation Index (NDVI)

The NDVI illustrates the viability to measure growth and the levels of vegetation in the target region. Here, we measured NDVI by applying equation (5).

$$NDVI = \frac{(NIR - RED)}{(NIR + RED)} \quad (5)$$

In this case, we used the values (-1) and (+1) for the NDVI index's minimum and maximum, respectively. Classes of NDVI that we mapped are as follows: (1) (-0.351)-(-0.064), (2) (-0.064)-(0.008), (3) (0.008)-(0.099), (4) (0.099)-(0.260), and (5) (0.260)-(0.759).

14. Rainfall

The onset of landslides is unquestionably influenced by the severity and length of rainfall.

In this work, the rainfall data was obtained from the different meteorological stations distributed over study regions (GSI meteorological data). We applied the inverse distance weighting (IDW) concept to achieve rainfall map, which was classified into the following classes: (1) 438–440, (2) 440–480, (3) 480–520, (4) and 520–560.

15. Lithology

Lithology is found to have the very strong impact on slope stability and bedrock types. To measure the susceptibility of various lithological formations causing landslides, in this work lithological units were extracted from GSI datasets available for public access, where the scale was taken as 1:100,000. The total lithological units were obtained from the different regions and were classified into 8 different classes.

16. Soil Texture

Soil texture influences permeability and cohesion characteristics of the soil, which can have the decisive impact on soil movement and hence landslides. By removing organic mats (for example, horizon C) and horizon A, landslides alter soil properties by exposing native material [84]. Soil texture changes occur as a result of landslides shifting or removing materials from different locations [85]. In order to quantify soil texture using the hydrometric technique, several soil samples were taken from different lithological units. Soil texture triangle was used to organise textures in this study. Here, we divided the soil map into five categories: (1) Silty Loam, (2) Clay Loam, (3) Loam, (4) Sandy Loam, and (5) Silty Clay.In addition to the characteristics already mentioned, such as the proximity to the fault, the river, the road, and the density of the fault, river, and road. That way, we could save 25 input features for our significant predictor test. The features that were collected were subsequently subjected to processing utilising the Wilcoxon Rank Sum Test and Bi-LSTM for learning and feature extraction. Presented below is a brief overview of the feature selection process that is driven by significant predictor tests.

B. Significant Predictor Test (SPT)

One of the predominant problems, which were not addressed by many researchers in landslides prediction domain is the retention and/or identification of the most significant influencing factors towards (landslides risk) prediction. Though, the input environmental data collected were in dozens to ensure computationally efficient and more time efficient prediction solution, we performed significant predictor test to retain the set of most vital features. In this work, significant predictor test applied correlation amongst the collected landslide inventory data (say, the derived influencing candidate parameters) to measure level of significance of each (influencing factor) parameter. In this case, we used the Wilcoxon Rank Sum technique to assess the degree of association between the collected environmental factors and the factors that had an impact. Each potential factor was treated as an independent variable, with the landslip prediction label serving as the dependent variable. We kept the parameters that had an impact greater than the level of significance (here, we used a level of significance of p=0.05) after we retrieved the level of significance for each feature element; we eliminated the others.

In this manner, the proposed model identified a set of 16 features representing the vital landslide factors which have been passed to the proposed cascaded hybrid deep model.

C. Hybrid Deep Model Driven Learning

In this research the emphasis is made on learning over both local as well as long-term dependency features from the identified landslide influencing factors and therefore a hybrid deep network is designed by cascading LSTM with Bi-LSTM network design. In

Economic Sciences
https://economic-sciences.com
ES (2025) 21(1), 153-173 | ISSN:1505-4683

this research, we demonstrated how the Agentic Workflow approach might improve LLMs' ability to recognise emotions in tweets written in more than one language. In addition to improving decision-making accuracy, asking LLMs to explain their decisions openly can help humans understand them better. Because it sheds light on how these complicated systems function, explainability is, in our opinion, very important in real-world applications. However, we need to be wary of the dangers of employing LLMs in subjective tasks; these models could be wrong but give the impression of being confident. In the future, we hope to investigate how Agentic Workflows can be used to a wider range of sentiment analysis and natural language processing domains.

The detailed discussion of the deployed LSTM and Bi-LSTM network in a cascade architecture is given in the subsequent sections.

A. LSTM Network

The vanishing effect and the inflating gradient are two issues that classical recurrent neural networks have, and the LSTM deep learning model was conceptually created to solve these problems. Input, forget, and output gates are the building blocks of long short-term memory (LSTM) circuits (Fig. 1). The forget gate f_t in the shown LSTM model (Fig. 1) determines whether to remember the information from the previous state (c_(t-1)) or throw it out.

To achieve it, the LSTM learns over the input (x_t) and the hidden state (h_{t-1}). Thus, the measured value often gives output as binary, (i.e., 0 or 1) signifying whether to retain or drop the information. In this case, the input gate (i_t) determines whether the cell's status should be set to 0 or 1 based on the levels of data associated with x_t and h_(t-1). The mathematical function on c_(t-1), f_t, and i_t is used to measure the cell state in Fig. 1, where c_t denotes the result. Here, the output gate (O_t) is responsible for updating the outcomes as 0 or 1 and controlling the flow of information from the current cell state to the concealed state. Assuming t is the current time and x_t is the input to the long short-term memory (LSTM), the previous hidden state (h_(t-1)) and corresponding previous cell-state (c_(t-1)) would be, respectively. Let c_t stand for the present state of the cell and h_t for the current output at the hidden state. Hence, this LSTM structure may be used to determine the different gate elements and their outputs according to (6-10).

$$f_t = sigmoid\left(W_{fx}x_t + W_{fh}h_{t-1} + b_f\right) \quad (6)$$

$$i_t = sigmoid(W_{ix}x_t + W_{ih}h_{t-1} + b_i) \quad (7)$$

$$c_t = c_{t-1} \odot f_t + i_t \odot tanh(W_{cx}x_t + W_{ch}h_{t-1} + b_c) \quad (8)$$

$$O_t = sigmoid(W_{ox}x_t + W_{ch}h_{t-1} + b_0) \quad (9)$$

$$h_t = O_t tanh(c_t) \quad (10)$$

In (6-10), $x_t \in R^n$ be the input landslide influencing factor's feature vector, $W \in R^{v*n}$, $b \in R^v$. In this case, the superscript variables v and n stand for the input vector's dimensions and the number of feature items in the input data, respectively.

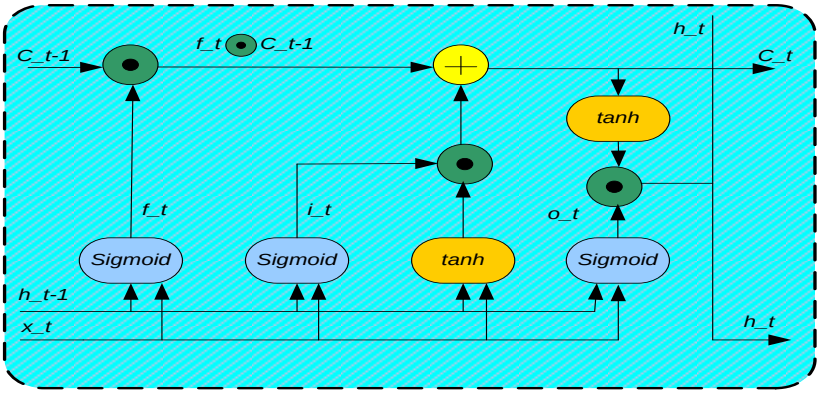

Fig. 1 LSTM network

Economic Sciences
https://economic-sciences.com
ES (2025) 21(1), 153-173 | ISSN:1505-4683

Literatures reveal that the classical recurrent neural networks including LSTM and CNN performs better for local feature extraction. On the contrary, in this work where we intend to exploit multiple correlated influencing factors for landslide prediction, learning their inherent or latent associations or dependency is inevitable to ensure reliable landslide prediction. Considering this fact, we designed a cascaded deep architecture by strategically amalgamating LSTM with Bi-LSTM network. In the proposed hybrid deep network (model), the LSTM was designed in such manner that the maximum pooling layer of the LSTM was replaced with BI-LSTM which learns over the LSTM extracted features to retain long-term dependency or global features for more accurate landslide prediction.

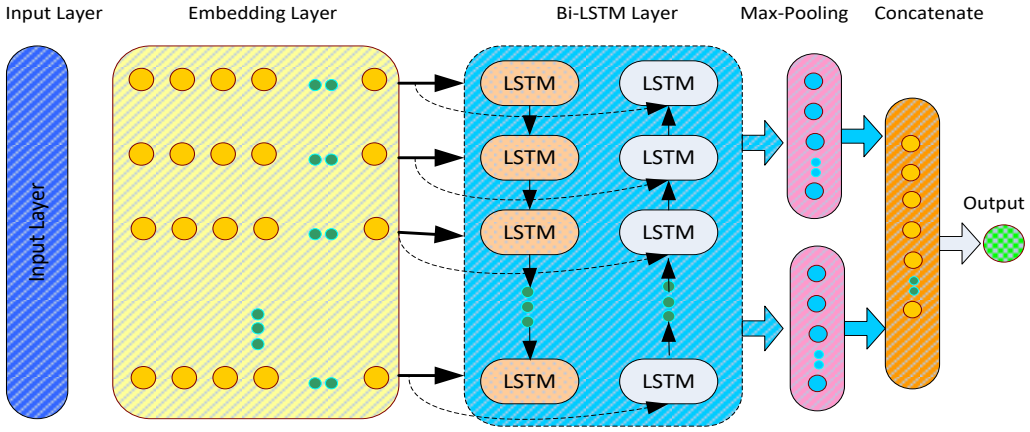

Fig. 2 Bi-LSTM Layer

To learn and classify, the created hybrid deep model uses both global and local features, much like a cascade model. The Bi-LSTM learns from the LSTM layer's outputs to produce finer-grained latent features, which are then combined at the global average pooling layer for classification and additional learning (at the Softmax layer). The following is a sample of the applied Bi-LSTM network's layers:

a. Input Layer

As stated above, Bi-LSTM being a supplementary layer substituted at the Max-pooling layer of (deployed) LSTM learns over the LSTM's extracted feature (say, the input vector x_t). Consider, w_1, $w_2, w_3, \dots, w_v$ be the number of features (say, the feature extracted from each landslides influencing factors) $D = d_1, d_2, d_3, \dots, d_m$. The elements i_1, i_2, i_3,..., i_v are all natural non-zero indices that contribute to the total. The components mentioned above use the symbols 1 and v to denote the first and last data indices, respectively. We provide a Bi-LSTM model that takes in landslip affecting factors or allied feature vectors in a sequential fashion with a predetermined window-size. Following this layer is an embedding layer, which, when stacked, produces an embedding matrix, as shown in (11). This layer converts each embedded index to a corresponding real-valued feature vector.

$$R = \begin{matrix} r_{1,1} & r_{1,2} & \cdots & r_{1,n} \\ r_{2,1} & r_{2,2} & \cdots & r_{2,n} \\ r_{3,1} & r_{3,2} & \cdots & r_{3,n} \\ \vdots & \vdots & \ddots & \vdots \\ r_{v-1,1} & r_{v-1,2} & \cdots & r_{v-1,n} \\ r_{v,1} & r_{v,1} & \cdots & r_{v,n} \end{matrix} \quad (11)$$

In equation (11), each row represents a different index that represents a component that can cause a unit landslip.

The dimension of the embedding matrix is $v * d$, with the dimension of the data v and the dense layer d. To generate the embedding vector, the proposed model assigned $d = 200$. The Bi-LSTM layer, which was assigned at the place of the maximum pooling layer of LSTM is briefed in the subsequent section.

1. Bi-LSTM Layer

Economic Sciences
https://economic-sciences.com
ES (2025) 21(1), 153-173 | ISSN:1505-4683

Although data can only travel forward in a native LSTM model, Bi-LSTM allows for both forward and backward data flow. In a Bi-LSTM network, in contrast to a traditional LSTM, the state at time t is dependent on both the data collected before t and the data collected after t.

Thus, the use of Bi-LSTM enabled learning over the long-range dependency amongst the input landslide influencing factor's features that achieved more semantically enriched feature. Each of the two LSTM units that make up the Bi-LSTM layer can process input vectors in either the forward or backward direction, as shown in Figure 2. Nevertheless, because we wanted to keep things simple, we only employed each LSTM for feature extraction in one direction, as shown in Figure 2. In this case, the forward LSTM takes data in from the left and processes it on the right, hence the corresponding hidden layer output is (12).

$$\vec{h}_t = LSTM\left(x_t, \vec{h}_{t-1}\right) \quad (12)$$

A backward LSTM's matching hidden layer data is retrieved in the following way: (13),

in contrast to a forward LSTM, which processes information in the left-to-right manner (Fig. 2).

$$\overleftarrow{h}_t = LSTM\left(x_t, \overleftarrow{h}_{t+1}\right) \quad (13)$$

Finally, the extracted features from both LSTM types were concatenated to yield the final composite feature, given as (14).

$$h_{t,Bi-LSTM} = \left[\vec{h}_t, \overleftarrow{h}_t\right] \quad (14)$$

2. *Global Average Max-Pooling Layer*

As we've already established, Bi-LSTM can learn over both short-term contextual features and long-term dependency relationships among the input features (like landslide influencing factors) because it keeps both local and global features (together with LSTM and Bi-LSTM outputs). In the deployed hybrid deep network, the features obtained from LSTM layer as well as Bi-LSTM layer were concatenated at the global average pooling (GAP) layer (Fig. 2). Thus, at the GAP layer, we retained high-resolution composite features which was passed to the flatten layer followed by the Softmax layer. Consider that the cumulative or composite feature vector be L_s and the number of convolutional kernels be B. In this case, applying B convolutional kernels and $2d$ dimensional output vector in Bi-LSTM were assigned the same value. In this manner, the generated feature vector (from, LSTM) be $H \in R^{(L\times d)\times 2d}$(say, the sliced vector), and the output of the LSTM be $H_{LSTM} = [C_1, C_2, \dots, C_n], C \in R^{l\times B}$. Similarly, the output from Bi-LSTM be $H_{t_Bi_{\mathrm{LSTM}}} = [h_1, h_2, \dots, h_L]$and $H_t \in R^{l\times 2d}$. In the proposed model, the GAP layer averaged the input vector H (15) to obtain feature points $L_s \in R^{2d}$, stating the feature representation of the complete input vectors.

$$H = Conc(H_{LSTM} + H_{Bi-LSTM}) \quad (15)$$

This approach enabled the avoidance of any probable over-fitting problem.

$$L_s = GAP(H) \quad (16)$$

Output Layer

The output of the GAP layer L_s (16) was projected as input to the output layer to perform two-class classification.

$$Loss_{Function} = -\frac{1}{m}\sum_{i}^{m}\Big(y_i * log\big(p(y_i)\big) + (1-y_i) * log\big(1-p(y_i)\big)\Big) \quad (17)$$

In equation (17), m, the input attributes, and p(y_i), the genuine labels, are represented. For landslip prediction, the cross-entropy function is shown by equation (17). Bear in mind that there is a very small discrepancy in the original data representing landslide impacting elements (for example, true labels in landslide risk data), but you can use the logarithmic function in cross-entropy to increase the distance between the data.

Because of this, the computation error can be reduced to a minimum.

The application of cross-entropy becomes critical since it guarantees that each landslide influencing element has a different weight, which is important because each component affects the landslide

probability in its own unique way. Consequently, it improves learning and produces more accurate results. To further accelerate convergence and guarantee that local minima or optima would likely occur during learning, the proposed cascaded hybrid deep model can also decide the direction of the fast gradient descent.

Using cross-entropy improves the accuracy of the likelihood of optimisation in the long run. Put otherwise, the chances of a landslide being close to one would be maintained, but the chances of a non-landslide staying close to zero would also be maintained. Accuracy and precision in classification can be enhanced. In light of the above, we used (17) in conjunction with the adaptive learning model ADAM, training it at a rate of 0.001, to establish a two-category classification system: 1-Landslide Probability YES and 0-Landslide Probability NO. What follows is a more in-depth analysis of the general findings and related conclusions from the simulation.

V. Results and Discussion

In sync with the goal to design a robust multi-parametric (environmental) sensitive landslide prediction system, in this paper a highly robust deep learning environment was designed. Though, to achieve superior efficiency and reliability, this work emphasized on both feature engineering as well as classification environment. Unlike classical researches where the authors have applied standalone feature (like, rainfall pattern [43]][49][50][59], slope [60]) or some other spatial features like slope, soil etc., this work amalgamated a total 17 distinct spatio-temporal features from the different landslide portfolio factors including geological, geomorphometric, soil, environmental and precipitation, etc. Noteworthy, the different influencing factors were obtained by processing rigorous feature significance analysis so as to ensure higher reliability. Functionally, the data were at first collected from the benchmarks like NASA meteorological details, followed by other secondary sources like Geological Survey of India (GSI), and other publicly availble details like Kaggle data, GitHub etc. Initially, a total of 107 environmental factors were identified. A number of key parameters were derived by applying different technologies such as GIS, GEE (Google Earth Engine), ArcGIS, SAGA etc. The collected data were later even processed for DEM analysis. Identifying a set of 25 environment parameters, we performed rank sum test as the significant predictor test that eventually retained a total of 16 most significant influencing factors having decisive impact on landslide risk prediction. In order to conduct further analysis, sixteen factors were taken into account. These factors include: slope angle, aspect, elevation above sea level, curvature, profile curvature, plan curvature, solar radiation, number of valleys, terrain ruggedness index, stream power index, topographic wetness index, length slope, topographic position index, land use, normalised difference vegetation index, soil, and rainfall.

Noticeably, to alleviate any likelihood of over-fitting and global optima over non-linear features, data normalization using Min-Max algorithm was performed. An LSTM and Bi-LSTM cascaded hybrid deep learning model was suggested, which would use normalised data representing the spatio-temporal aspects of various environmental parameters. By strategically replacing LSTM's Max-pooling layer with B-LSTM, we were able to maintain both local and global characteristics, or long-term dependencies, in the suggested hybrid deep learning model, allowing for greater learning. The LSTM model's architecture includes a dense layer, an average pooling layer, a batch normalisation layer, and an activation function that uses ReLU.

Moreover, the learning rate assigned was 0.001, while the learning optimizer was deployed as ADAM. Finally, the extracted features from LSTM and Bi-LSTM were trained over Softmax classifier layer to perform risk prediction. In sync with binary classification problem (i.e., Positive Landslide Risk (‘1’) and Negative Landslide Risk (‘0’)), we applied binary cross-entropy information for classification. The proposed model was implemented over Python Notebook platform, where the simulation was done with different Pythons advanced libraries including TensorFlow, Keras etc. An Intel i5 processor, 8 GB of RAM, and a 3.00 GHz CPU were utilised to execute the simulation on a computer system secured by Microsoft operating system.

As a binary classification task, the suggested model's performance was evaluated by obtaining a confusion

Economic Sciences
https://economic-sciences.com
ES (2025) 21(1), 153-173 | ISSN:1505-4683

matrix that included the following columns: TP, TN, FP, and FN. Other statistical performance metrics such as recall, accuracy, precision, and F-Measures were derived from the parameters of the confusion matrix. Table I provides the formulas for measuring these variables.

Table I. Performance Parameters

Parameter	**Mathematical Expression**	**Definition**
Accuracy	$\frac{(TN+TP)}{(TN+FN+FP+TP)}$	Indicates the fraction of classes (landslide probability class) that were accurately classified out of all the classes.
Precision	$\frac{TP}{(TP+FP)}$	Indicates how well the results hold up when measured again under the same conditions.
Recall	$\frac{TP}{(TP+FN)}$	It specifies the number of pertinent things that need to be located.
F-Score	$2.(Recall.Precision)/(Recall+Precision)$	A single score is produced by combining the recall and precision numerical values; this score is defined as the harmonic mean of the two.

To examine whether the proposed model, especially with the LSTM and Bi-LSTM yields superior efficiency, we trained both models (i.e., LSTM as well as hybrid LSTM-Bi-LSTM together with 100 epochs) independently over the extracted feature vector (the Min-Max normalized features pertaining to the 16 selected landslide influencing factors). The primary goal here was to see if the suggested hybrid deep learning environment might outperform more traditional RNNs, such as LSTM. You can see the outcomes of the simulation in Table II.

Table II Relative (Intra-Model) performance

Model	**Accuracy (%)**	**Precision (%)**	**Recall (%)**	**F-Measure (%)**
LSTM	91.52	92.11	92.65	92.38
Hybrid *LSTM-Bi-LSTM	96.38	95.19	95.93	95.56
*Proposed Method				

Figure 4 shows the visual representation of the outcomes. Looking at the data in Table II, it's clear that the suggested hybrid deep model (let's call it an LSTM-Bi-LSTM network) outperforms the traditional LSTM based method with an accuracy of 96.38%. The suggested hybrid deep learning model's capacity to learn dependent variables over the long run makes this a viable contribution. In a similar vein, the LSTM and Bi-LSTM models attained 92.11%, 92.63%, 92.38%, and 95.56% in terms of recall, accuracy, and F-Measure (in percentiles), respectively.

Economic Sciences
https://economic-sciences.com
ES (2025) 21(1), 153-173 | ISSN:1505-4683

It signifies that the proposed hybrid deep driven landslide prediction model exhibits superior performance than the classical recurrent neural network method (i.e., LSTM). The F-Measure which indicates reliability of the system too is found almost 0.9666, which is higher than 0.95, and hence confirms very good (say, reliable) performance by the proposed model.

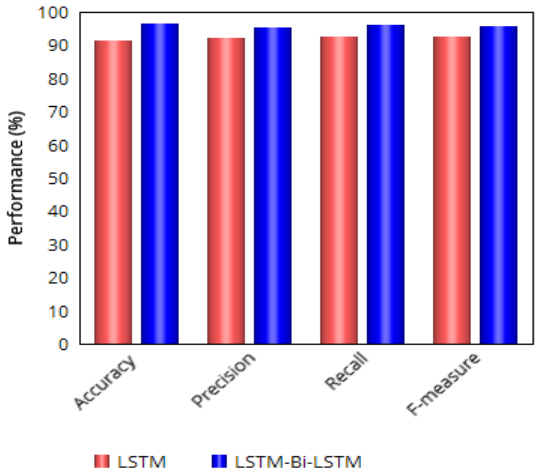

Fig. 4 Relative Intra-Model performance

In addition to the above discussed performance parameters, we assessed error profile of the learning models (i.e., LSTM and hybrid LSTM + Bi-LSTM). We assessed the error profile using the root-mean-square error (RMSE) and the mean-average error (MAE).

The simulation results obtained are given in Table III.

Table III Error performance

Model	**MAE**	**RMSE**
LSTM	4.721	2.152
Hybrid *LSTM-Bi-LSTM	0.1109	0.1860
*Proposed Method		

The error performance results (Table III) too confirms that the proposed hybrid deep model-based landslide prediction model exhibits MAE and RMSE of 0.1105 and 0.0060, respectively. On the contrary, the classical LSTM-based learning model exhibited MAE and RMSE of 4.721 and 2.152, respectively. Evidence of the suggested hybrid deep learning model's resilience in landslip risk prediction is presented. According to the results that have been already mentioned, the suggested LSTM and Bi-LSTM hybrid deep learning landslide prediction model has the potential to be very useful for landslide prediction.

We compared the suggested landslip risk prediction model's performance against that of other, more established methods, particularly those that made use of machine learning and deep learning techniques, in order to characterise inter-model performance. Taking into account a recent study by Utomo et al. [46] that utilised LSTM networks for landslip prediction, the best accuracy achieved was 90%, which is over 6.38 percentage points lower than the suggested model's 96.68% accuracy.

This result inference clearly indicates that though LSTM perform better over non-linear pattern; however, the native architecture lacks learning ability of long-term dependency or global features. However, the suggested hybrid model (i.e., cascading LSTM with Bi-LSTM) is able to efficiently learn over both

local and global data, allowing it to achieve a higher accuracy of 96.68%. This proves that the proposed model is better than the current one [46].

Considering a recent work by Xing et al. [77] applied LSTM model for landslides displacement measurement. Though, the authors applied LSTM with Softmax classifier, additionally, they assessed their feature efficacy with SVM and extreme learning methods. Interestingly, with LSTM the authors achieved RMSE and MAE of 7.28%, and 6.02%, respectively, which is significantly higher than our proposed model (RMSE= 0.1109, MAE=0.1860). In their model, SVM and ELM too exhibited RMSE of 8.94 and 7.45, and MAE of 8.42 and 7.01, respectively. The overall results infer that the proposed (say, hybrid deep model) achieves superior over the existing standalone LSTM or other machine learning methods for landslide risk prediction. To be noted, in this work the most significant features having decisive impact on the landslide risk assessment were considered and hence the superior performance seems relevant over the other state-of-arts. The authors in [38] too applied a robust cascade parallel neural network by using LSTM with conditional random field (CRF). After doing a thorough evaluation, they found that the proposed model could obtain a true positive rate of around 76%, which is much lower.

Though, their area under curve performance approached to almost 86%; yet, it falls below our model which can have the same performance output more than 95%. It confirms that the proposed hybrid deep model can perform superior over other state-of-art hybrid deep architectures like LSTM-CRF. In [43], Li et al. applied GEE derived rainfall information to perform landslide susceptibility mapping by using ensemble learning model. Undeniably, their area under curve performance of almost 97% looks similar to our approach; however, unlike standalone rainfall-based prediction our proposed model applied other spatio-temporal parameters as well, and hence contributes more reliable solution. Ghorbanzadeh et al. [78] applied a modified residual network for landslide prediction, where they achieved the highest precision of 73.44%, recall 80.33%, F1-score 76.56%, which are significantly lower than our proposed model. When it came to mapping the likelihood of landslidesFor their study, Zhang et al. [79] compared a number of ML and deep learning methods. For landslip prediction, they created a deep learning model named landslip net (LSNet) that achieved 95% accuracy, 95.1% precision, and an F1-score of 0.951. We present a model that outperforms this one by more than 2%. The results displayed above prove that the proposed methodology can outperform other cutting-edge approaches to landslip risk prediction.

VI. Conclusion

A landslip prediction system powered by a hybrid-deep network is presented in this paper.

The suggested model aimed to enhance the computing environment in addition to the features.

As feature environment numerous influencing factors were obtained from the landslide inventory data. To ensure optimality of features, Wilcoxon Rank sum algorithm driven significant predictor test was applied over the input inventory data that eventually selected the optimal set of influencing factors towards landslide prediction. In particular, sixteen factors were identified by the proposed feature selection model as having an impact. Sunlight, altitude above sea level, orientation, slope angle, curvature, profile curvature, plan curvature, terrain ruggedness index, stream power index, topographic wetness index, length slope, topographic position index, land use, normalised difference vegetation index, soil, and rainfall are all factors to consider.

The input to the hybrid deep network, which includes LSTM and Bi-LSTM, was the features that were extracted. Instead of using CNNs or LSTMs, which are classical feature extraction methods that can only use word-level local features, this study used Bi-LSTMs, which were trained over LSTM extracted features to retain long-term dependency, to extract features. By training on both local and global variables (such as the interdependence of the influencing elements across time), the LSTM-Bi-LSTM model was able to achieve superior learning and classification performance. The suggested model achieves landslip prediction accuracy of 96.38%, precision of 95.19%, recall of 95.33%, and F-Measure of 95.56%, as shown in the simulation over benchmarks. The suggested model is robust, as shown by the mean average error of 0.1109 and the root mean square error value of 0.1860. Of the methods for

mapping and predicting landslip susceptibility that have been established thus far, the simulation results were determined to be the most effective. The suggested model is reliable for landslip prediction in real-time, according to the error profiling results (i.e., MAE 0.0862 and RMSE 0.1358).

VII. Reference

1. A. Joshi, J. Grover, D. P. Kanungo, and R. K. Panigrahi, ``Edge assisted reliable landslide early warning system," in Proc. IEEE 16th India Council Int. Conf. (INDICON), Dec. 2019, pp. 1_4.
2. M. Li, M. Zhu, Y. Hec, Z. He, N.Wang, Z. Zheng, and G. Zhou, ``Warning of rainfall-induced landslide in bazhou district," in Proc. IEEE Int. Geosci. Remote Sens. Symp. (IGARSS), Sep. 2020, pp. 6879_6882.
3. Shahabi, H.; Khezri, S.; Ahmad, B.B.; Hashim, M. Landslide susceptibility mapping at central Zab basin, Iran: A comparison between analytical hierarchy process, frequency ratio and logistic regression models. Catena 2014, 115, 55–70.
4. Tien Bui, D.; Pradhan, B.; Lofman, O.; Revhaug, I.; Dick, O.B. Landslide susceptibility assessment in the Hoa Binh province of Vietnam: A comparison of the Levenberg–Marquardt and Bayesian regularized neural networks. Geomorphology 2012, 171–172, 12–29.
5. Moayedi, H.; Osouli, A.; Tien Bui, D.; Foong, L.K. Spatial Landslide Susceptibility Assessment Based on Novel Neural-Metaheuristic Geographic Information System Based Ensembles. Sensors 2019, 19, 4698.
6. Amatya, P.; Kirschbaum, D.; Stanley, T. Use of Very High-Resolution Optical Data for Landslide Mapping and Susceptibility Analysis along the Karnali Highway, Nepal. Remote Sens. 2019, 11, 2284.
7. Zhao, C.; Lu, Z. Remote Sensing of Landslides—A Review. Remote Sens. 2018, 10, 279.
8. Youssef, A.M.; Pourghasemi, H.R.; Pourtaghi, Z.S.; Al-Katheeri, M.M. Landslide susceptibility mapping using random forest, boosted regression tree, classification and regression tree, and general linear models and comparison of their performance at Wadi Tayyah Basin, Asir Region, Saudi Arabia. Landslides 2015, 13, 839–856.
9. Wang, Q.; Wang, Y.; Niu, R.; Peng, L. Integration of Information Theory, K-Means Cluster Analysis and the Logistic Regression Model for Landslide Susceptibility Mapping in the Three Gorges Area, China. Remote Sens. 2017, 9, 938.
10. Erener, A.; Mutlu, A.; Sebnem Düzgün, H. A comparative study for landslide susceptibility mapping using GIS-based multi-criteria decision analysis (MCDA), logistic regression (LR) and association rule mining (ARM). Eng. Geol. 2016, 203, 45–55.
11. Sevgen, E.; Kocaman, S.; Nefeslioglu, H.A.; Gokceoglu, C. A novel performance assessment approach using photogrammetric techniques for landslide susceptibility mapping with logistic regression, ann and random forest. Sensors 2019, 19, 3940.
12. Tien Bui, D.; Shahabi, H.; Shirzadi, A.; Chapi, K.; Alizadeh, M.; Chen, W.; Mohammadi, A.; Ahmad, B.B.; Panahi, M.; Hong, H.; et al. Landslide detection and susceptibility mapping by airsar data using support vector machine and index of entropy models in cameron highlands, malaysia. Remote Sens. 2018, 10, 1527.
13. Devkota, K.C.; Regmi, A.D.; Pourghasemi, H.R.; Yoshida, K.; Pradhan, B.; Ryu, I.C.; Dhital, M.R.; Althuwaynee, O.F. Landslide susceptibility mapping using certainty factor, index of entropy and logistic regression models in GIS and their comparison at Mugling–Narayanghat road section in Nepal Himalaya. Nat. Hazards 2012, 65, 135–165.
14. Chen, W.; Li, W.; Chai, H.; Hou, E.; Li, X.; Ding, X. GIS-based landslide susceptibility mapping using analytical hierarchy process (AHP) and certainty factor (CF) models for the Baozhong region of Baoji City, China. Environ. Earth Sci. 2015, 75, 63.
15. Hasekiˇ gulları, G.D.; Ercanoglu, M. A new approach to use AHP in landslide susceptibility mapping: A case study at Yenice (Karabuk, NW Turkey). Nat. Hazards 2012, 63, 1157–1179.
16. Nguyen, T.T.N.; Liu, C.-C. A New Approach Using AHP to Generate Landslide Susceptibility Maps in the Chen-Yu-LanWatershed, Taiwan. Sensors 2019, 19, 505.
17. Wang, Y.;Wu, X.; Chen, Z.; Ren, F.; Feng, L.; Du, Q. Optimizing the predictive ability of machine learning methods for landslide susceptibility mapping using smote for lishui city in zhejiang province, china. Int. J. Environ. Res. Public Health 2019, 16, 368.

18. Yu, X.; Wang, Y.; Niu, R.; Hu, Y. A combination of geographically weighted regression, particle swarm optimization and support vector machine for landslide susceptibility mapping: A case study at Wanzhou in the Three Gorges Area, China. Int. J. Environ. Res. Public Health 2016, 13, 487.
19. Chen,W.; Hong, H.; Panahi, M.; Shahabi, H.;Wang, Y.; Shirzadi, A.; Pirasteh, S.; Alesheikh, A.A.; Khosravi, K.; Panahi, S. Spatial prediction of landslide susceptibility using GIS-based data mining techniques of anfis with whale optimization algorithm (woa) and grey wolf optimizer (gwo). Appl. Sci. 2019, 9, 3755.
20. Truong, X.L.; Mitamura, M.; Kono, Y.; Raghavan, V.; Yonezawa, G.; Truong, X.Q.; Do, T.H.; Tien Bui, D.; Lee, S. Enhancing Prediction Performance of Landslide Susceptibility Model Using Hybrid Machine Learning Approach of Bagging Ensemble and Logistic Model Tree. Appl. Sci. 2018, 8, 1046.
21. Conoscenti, C.; Ciaccio, M.; Caraballo-Arias, N.A.; Gómez-Gutiérrez,Á.; Rotigliano, E.; Agnesi,V. Assessment of susceptibility to earth-flow landslide using logistic regression and multivariate adaptive regression splines: A case of the Belice River basin (western Sicily, Italy). Geomorphology 2015, 242, 49–64.
22. Felicísimo, Á.M.; Cuartero, A.; Remondo, J.; Quirós, E. Mapping landslide susceptibility with logistic regression, multiple adaptive regression splines, classification and regression trees, and maximum entropy methods: A comparative study. Landslides 2012, 10, 175–189.
23. Zhu, A.X.; Wang, R.; Qiao, J.; Qin, C.-Z.; Chen, Y.; Liu, J.; Du, F.; Lin, Y.; Zhu, T. An expert knowledge-based approach to landslide susceptibility mapping using GIS and fuzzy logic. Geomorphology 2014, 214, 128–138.
24. Huang, F.; Huang, J.; Jiang, S.; Zhou, C. Landslide displacement prediction based on multivariate chaotic model and extreme learning machine. Eng. Geol. 2017, 218, 173–186.
25. Bui, D.T.; Moayedi, H.; Kalantar, B.; Osouli, A.; Pradhan, B.; Nguyen, H.; Rashid, A.S.A. A novel swarm intelligence—harris hawks optimization for spatial assessment of landslide susceptibility. Sensors 2019, 19, 3590.
26. Li, D.; Huang, F.; Yan, L.; Cao, Z.; Chen, J.; Ye, Z. Landslide Susceptibility Prediction Using Particle-Swarm-Optimized Multilayer Perceptron: Comparisons with Multilayer-Perceptron-Only, BP Neural Network, and Information Value Models. Appl. Sci. 2019, 9, 3664.
27. Tsangaratos, P.; Ilia, I. Landslide susceptibility mapping using a modified decision tree classifier in the Xanthi Perfection, Greece. Landslides 2015, 13, 305–320.
28. Shirzadi, A.; Soliamani, K.; Habibnejhad, M.; Kavian, A.; Chapi, K.; Shahabi, H.; Chen, W.; Khosravi, K.; Thai Pham, B.; Pradhan, B. Novel GIS based machine learning algorithms for shallow landslide susceptibility mapping. Sensors 2018, 18, 3777.
29. Park, S.-J.; Lee, C.-W.; Lee, S.; Lee, M.-J. Landslide Susceptibility Mapping and Comparison Using Decision Tree Models: A Case Study of Jumunjin Area, Korea. Remote Sens. 2018, 10, 1545. [CrossRef]
30. Chen, W.; Xie, X.; Wang, J.; Pradhan, B.; Hong, H.; Bui, D.T.; Duan, Z.; Ma, J. A comparative study of logistic model tree, random forest, and classification and regression tree models for spatial prediction of landslide susceptibility. Catena 2017, 151, 147–160.
31. Lai, J.-S.; Tsai, F. Improving GIS-based landslide susceptibility assessments with multi-temporal remote sensing and machine learning. Sensors 2019, 19, 3717.
32. Park, S.; Kim, J. Landslide Susceptibility Mapping Based on Random Forest and Boosted Regression Tree Models, and a Comparison of Their Performance. Appl. Sci. 2019, 9, 942.
33. Dai, S.; Niu, D.; Han, Y. Forecasting of power grid investment in China based on support vector machine optimized by di_erential evolution algorithm and grey wolf optimization algorithm. Appl. Sci. 2018, 8, 636.
34. Roy, J.; Saha, S.; Arabameri, A.; Blaschke, T.; Bui, D.T. A novel ensemble approach for landslide susceptibility mapping (LSM) in darjeeling and kalimpong districts, west bengal, india. Remote Sens. 2019, 11, 2866.
35. Huang, F.; Yin, K.; Zhang, G.; Zhou, C.; Zhang, J. Landslide groundwater level time series prediction based on phase space reconstruction and wavelet analysis-support vector machine optimized by PSO algorithm. Earth Sci.-J. China Univ. Geosci. 2015, 40, 1254–1265.
36. Roodposhti, M.S.; Aryal, J.; Pradhan, B. A novel rule-based approach in mapping landslide susceptibility. Sensors 2019, 19, 2274.

37. Nsengiyumva, J.B.; Luo, G.; Nahayo, L.; Huang, X.; Cai, P. Landslide Susceptibility Assessment Using Spatial Multi-Criteria Evaluation Model in Rwanda. Int. J. Environ. Res. Public Health 2018, 15, 243.
38. L. Zhu, L. Huang, L. Fan, J. Huang, F. Huang, J. Chen, Z. Zhang and Y. Wang, "Landslide Susceptibility Prediction Modelling Based on Remote Sensing and a Novel Deep Learning Algorithm of a Cascade-Parallel Recurrent Neural Network", Sensors 2020, 20, 1576.
39. Tien Bui, D.; Hoang, N.D.; Martinez-Alvarez, F.; Ngo, P.T.; Hoa, P.V.; Pham, T.D.; Samui, P.; Costache, R. A novel deep learning neural network approach for predicting flash flood susceptibility: A case study at a high frequency tropical storm area. Sci. Total Environ. 2019, 701, 134413.
40. Chen, Y.; Lin, Z.; Zhao, X.; Wang, G.; Gu, Y. Deep Learning-Based Classification of Hyperspectral Data. IEEE J. Sel. Top. Appl. Earth Obs. Remote Sens. 2014, 7, 2094–2107.
41. Liu, Y.; Wu, L. Geological Disaster Recognition on Optical Remote Sensing Images Using Deep Learning. Procedia Comput. Sci. 2016, 91, 566–575.
42. Huang, F.; Zhang, J.; Zhou, C.;Wang, Y.; Huang, J.; Zhu, L. A deep learning algorithm using a fully connected sparse autoencoder neural network for landslide susceptibility prediction. Landslides 2020, 17, 217–229.
43. B. Li, K. Liu, M. Wang, Q. He, Z. Jiang, W. Zhu and N. Qiao, "Global Dynamic Rainfall-Induced Landslide Susceptibility Mapping Using Machine Learning", Remote Sens. 2022, 14, 5795.
44. J. Remondo, J. Bonachea, and A. Cendrero, ``A statistical approach to landslide risk modelling at basin scale: From landslide susceptibility to quantitative risk assessment," Landslides, vol. 2, no. 4, pp. 321_328, 2005.
45. F. Tan, J. Yu, Y.-Y. Jiao, D. Lin, J. Lv, and Y. Cheng, ``Rapid assessment of landslide risk level based on deep learning," Arabian J. Geosci., vol. 14, no. 3, pp. 1_10, Feb. 2021.
46. P. Goyes-Peña_el and A. Hernandez-Rojas, ``Landslide susceptibility index based on the integration of logistic regression and weights of evidence: A case study in Popayan, Colombia," Eng. Geol., vol. 280, Jan. 2021, 105958.
47. D. Utomo, L.-C. Hu, and P.-A. Hsiung, ``Deep neural network-based data reconstruction for landslide detection," in Proc. IEEE Int. Geosci. Remote Sens. Symp. (IGARSS), Sep. 2020, pp. 3119_3122.
48. Z.-Q. Liu, D. Guo, S. Lacasse, J.-H. Li, B.-B. Yang, and J.-C. Choi, ``Algorithms for intelligent prediction of landslide displacements," J. Zhejiang Univ. Sci. A, vol. 21, no. 6, pp. 412_429, Jun. 2020.
49. S. Srivastava, N. Anand, S. Sharma, S. Dhar, and L. K. Sinha, ``Monthly rainfall prediction using various machine learning algorithms for early warning of landslide occurrence," in Proc. Int. Conf. for Emerg. Technol. (INCET), Jun. 2020, pp. 1_7.
50. C. C. Khaing and T. L. L. Thein, ``Prediction of rainfall based on deep learning and Internet of Things to prevent landslide," in Proc. IEEE 9th Global Conf. Consum. Electron. (GCCE), Oct. 2020, pp. 190_191.
51. M. Di Napoli, F. Carotenuto, A. Cevasco, P. Confuorto, D. Di Martire, M. Firpo, G. Pepe, E. Raso, and D. Calcaterra, ``Machine learning ensemble modelling as a tool to improve landslide susceptibility mapping reliability," Landslides, vol. 17, no. 8, pp. 1897_1914, Apr. 2020.
52. J. Dou, A. P. Yunus, D. T. Bui, A. Merghadi, M. Sahana, Z. Zhu, C.-W. Chen, Z. Han, and B. T. Pham, ``Improved landslide assessment using support vector machine with bagging, boosting, and stacking ensemble machine learning framework in a mountainous watershed, Japan," Landslides, vol. 17, no. 3, pp. 641_658, Mar. 2020.
53. Z. Liang, C. Wang, and K. U. J. Khan, ``Application and comparison of different ensemble learning machines combining with a novel sampling strategy for shallow landslide susceptibility mapping," Stochastic Environ. Res. Risk Assessment, vol. 35, no. 6, pp. 1243_1256, Jun. 2021.
54. Z. Ma, G. Mei, and F. Piccialli, ``Machine learning for landslides prevention: A survey," Neural Comput. Appl., pp. 10881_10907, Nov. 2020.
55. K. Liao, Y.Wu, F. Miao, L. Li, and Y. Xue, ``Using a kernel extreme learning machine with grey wolf optimization to predict the displacement of step-like landslide," Bull. Eng. Geol. Environ., vol. 79, no. 2, pp. 673_685, 2020.
56. H. Li, Q. Xu, Y. He, and J. Deng, ``Prediction of landslide displacement with an ensemble-based

extreme learning machine and copula models," Landslides, vol. 15, no. 10, pp. 2047_2059, May 2018.
57. F. Huang, K. Yin, G. Zhang, L. Gui, B. Yang, and L. Liu, ``Landslide displacement prediction using discrete wavelet transform and extreme learning machine based on chaos theory," Environ. Earth Sci., vol. 75, no. 20, pp. 1_18, Oct. 2016.
58. Y. Cao, K. Yin, D. E. Alexander, and C. Zhou, ``Using an extreme learning machine to predict the displacement of step-like landslides in relation to controlling factors," Landslides, vol. 13, no. 4, pp. 725_736, Jun. 2015.
59. C. Lian, Z. Zeng,W. Yao, and H. Tang, ``Extreme learning machine for the displacement prediction of landslide under rainfall and reservoir level," Stochastic Environ. Res. Risk Assessment, vol. 28, 8, pp. 1957_1972, 2014.
60. P. Chaturvedi, S. Srivastava, and N. Tyagi, ``Prediction of landslide deformation using back-propagation neural network," in Proc. IEEE Workshop Comput. Intell., Theories, Appl. Future Directions (WCI), Dec. 2015, pp. 1_5.
61. D. Zhang, J. Yang, F. Li, S. Han, L. Qin and Q. Li, "Landslide Risk Prediction Model Using an Attention-Based Temporal Convolutional Network Connected to a Recurrent Neural Network," in IEEE Access, vol. 10, pp. 37635-37645, 2022.
62. E. O. Yilmaz, A. Teke and T. Kavzoglu, "Performance Evaluation of Depthwise Separable CNN and Random Forest Algorithms for Landslide Susceptibility Prediction," IGARSS 2022 - 2022 IEEE International Geoscience and Remote Sensing Symposium, 2022, pp. 5477-5480.
63. C. Xu, K. Huang, C. Wei and Y. Lin, "Landslide Displacement Prediction Based on Variational Mode Decomposition and LSTM," 2022 20th Intl. Conf. on Optical Communications and Networks (ICOCN), 2022, pp. 1-3.
64. A. L. Achu, G. Gopinath and S. U, "Landslide susceptibility modelling using deep-learning and machine-learning methods-A study from southern Western Ghats, India," 2021 IEEE International India Geoscience and Remote Sensing Symposium (InGARSS), 2021, pp. 360-364.
65. M. Mubashar, G. M. Khan and R. Khan, "Landslide Prediction Using Long Short-Term Memory (LSTM)Neural Network on time series data in Pakistan," 2021 Intl. Conf. on Artificial Intel. (ICAI), 2021, pp. 175-181.
66. Y. Liu, X. Chi, X. Jia and M. Sun, "A Deep Learning Approach Using Gated Recurrent Unit for Prediction of Landslide Displacement Based on Spatial-Temporal Features of Multi-Monitoring Points," 2021 China Automation Congress (CAC), 2021, pp. 6936-6940.
67. Guzzetti, F.; Carrara, A.; Cardinali, M.; Reichenbach, P. Landslide hazard evaluation: A review of current techniques and their application in a multi-scale study, Central Italy. Geomorphology 1999, 31, 181–216.
68. Galli, M.; Ardizzone, F.; Cardinali, M.; Guzzetti, F.; Reichenbach, P. Comparing landslide inventory maps. Geomorphology 2008, 94, 268–289.
69. Asadi, M.; Goli Mokhtari, L.; Shirzadi, A.; Shahabi, H.; Bahrami, S. A comparison study on the quantitative statistical methods for spatial prediction of shallow landslides (case study: Yozidar-Degaga Route in Kurdistan Province, Iran). Environ. Earth Sci. 2022, 81, 51.
70. Dehnavi, A.; Aghdam, I.N.; Pradhan, B.; Varzandeh, M.H.M. A new hybrid model using step-wise weight assessment ratio analysis (SWARA) technique and adaptive neuro-fuzzy inference system (ANFIS) for regional landslide hazard assessment in Iran. Catena 2015, 135, 122–148.
71. Hunter, G.; Fell, R. Travel distance angle for “rapid” landslides in constructed and natural soil slopes. Can. Geotech. J. 2003, 40, 1123–1141.
72. Ayalew, L.; Yamagishi, H.; Marui, H.; Kanno, T. Landslides in Sado Island of Japan: Part II. GIS-based susceptibility mapping with comparisons of results from two methods and verifications. Eng. Geol. 2005, 81, 432–445.
73. Bhandary, N.P.; Dahal, R.K.; Timilsina, M.; Yatabe, R. Rainfall event-based landslide susceptibility zonation mapping. Nat. Hazards 2013, 69, 365–388.
74. Mandal, S.; Maiti, R. Semi-Quantitative Approaches for Landslide Assessment and Prediction; Springer: Berlin/Heidelberg, Germany, 2015.
75. Minár, J.; Evans, I.S.; Jenˇco, M. A comprehensive system of definitions of land surface (topographic) curvatures, with implications for their application in geoscience

modelling and prediction. Earth Sci. Rev. 2020, 211, 103414.
76. Sidle, R.C.; Ochiai, H. Landslides Processes, Prediction, and Land Use. Water Resources Monograph 18; American Geophysical Union: Washington, DC, USA, 2006; pp. 322–326.
77. Xing, J Yue, C Chen, "Interval Estimation of Landslide Displacement Prediction Based on Time Series Decomposition and Long Short-Term Memory Network", IEEE Access, Vol. 8, 2020, pp. 3187-3196.
78. [78] O. Ghorbanzadeh, H. Shahabi, A. Crivellari, S. Homayouni, T. Blaschke, P. Ghamisi, "Landslide detection using deep learning and object-based image analysis" Landslides, 2022, Vol. 19, pp. 929–939.
79. [79] T. Zhang, Y. Li, T. Wang, H. Wang, T. Chen, Z. Sun, D. Luo, C. Li and L. Han, "Evaluation of different machine learning models and novel deep learning-based algorithm for landslide susceptibility mapping", Geoscience Letters (Springer Open), 2022, Vol. 9, Issue. 26, pp. 1-16.